# Coastal vulnerability to tsunami impacts and modelling SWI in aquifers situated in the most vulnerable areas

Daniel Zamrsky

Internship report

Deltares, WUR

26/08/2013

# Contents

# 1. Introduction

## 1.1. Background

Tsunami events in recent year (2004 in Sumatra and 2011 in Japan) affected large areas and caused death of thousands of people, while also destroying infrastructure in the impacted regions. Several studies (Chidambaram et al. 2010) and (Violette et al. 2009) dealt with groundwater salinization in coastal aquifers caused by inundation due the tsunami wave. Despite a generally short time of inundation, the latter still results in contamination of groundwater (Violette et al. 2009).

Coastal areas provide a source of fresh groundwater for more than one billion people resulting in large groundwater extraction rates in the densely populated areas (Ferguson et al. 2012). Damage caused by a tsunami in these areas can have a large influence on groundwater systems, where the process of recovering from such an event can be very slow (Karen G. Villholth et al. 2011). The coastal population often relies on groundwater extraction based on a system of shallow wells; these can be severely impacted by tsunami waves (Karen G. Villholth et al. 2011).

A study by (G.H.P. Oude Essink et al. 2005) focused on numerical modelling of salt water intrusion (SWI) into the coastal aquifers and its potential effects on the water quality. The process of SWI depends on multiple parameters which can be hard to estimate on a global scale due to data unavailability (e.g. for hydraulic conductivities).

A global coastal database (DIVA) assessing vulnerability to sea level rise was developed in previous years under the DINAS-COAST project (Hinkel et al. 2003, Vafeidis et al. 2008). Covering the whole globe, it provides access to various data in areas where detailed information are still not yet available. Due to the rather coarse resolution of the data used it is not suitable for analysis on local scales but can serve as a tool for depicting the most vulnerable areas to sea level rise where further detailed analysis should be conducted (Vafeidis et al. 2008).

First global tsunami hazard and population exposure study was performed by Løvholt et al. (2012) focusing on development of a method for obtaining reasonable estimates of maximum water levels inflicted by a tsunami event. This is achieved by a thorough literature study and scenario simulations. The term tsunami hazard at a specific location is defined as annual probability of exceeding a specific run-up value (Løvholt et al. 2012). Vulnerability is not included in the analysis of this study due to its geographical extent and scenario based methodology. On the contrary, our study is focused on determining aerial coastal vulnerability on global scale to assess tsunami impacts from groundwater point of view, as explained in following section.

## 1.2. Aim of the study

Tsunami events can have severe impacts on the groundwater resources in the rather densely populated coastal areas. Highlighting potentially vulnerable areas to these negative impacts on a global scale could provide a valuable tool for coastal management, risk assessment and evacuation planning. This study is focused on developing a global database determining vulnerability to tsunami impacts on the coastal areas. Once these areas are located a numerical modelling of SWI into coastal aquifers is performed. The results could be useful in coastal management or evacuation planning.

## 1.3. Vulnerability definition

The term “vulnerability” is largely used in various research fields, a need for its clear definition is important for a better understanding of this study. A study by Füssel (2007) describes the use of this term and suggests a generally applicable framework that can be used in climate change research. The term vulnerability needs to be used with reference to a particular situation and should be described using four dimensions (Füssel 2007). Using this method the term vulnerability in this study is defined as vulnerability of fresh groundwater supplies in the coastal areas of the world to the tsunami inundation impacts.

# 2. Available global datasets

## 2.1. SRTM

Digital elevation model (DEM) data are the core of this study as the topographical parameters such as elevation, topographic slope and distance to coast are very important for the vulnerability assessment. The SRTM (Shuttle Radar Topography Mission) dataset was obtained from CGIAR-CSI server (http://srtm.csi.cgiar.org). This version includes interpolation of the voids that are present in the original SRTM dataset. The pixel size of the SRTM is 90m and covers the latitudes between 60°N and 54°S latitudes (see Figure 2-1). (Reuter et al. 2007)

Disadvantage of this dataset is a vertical error which is ≤16m of absolute vertical accuracy and ≤10m relative vertical high accuracy (NASA 2005), still, for assessment on a global scale it is a useful tool.

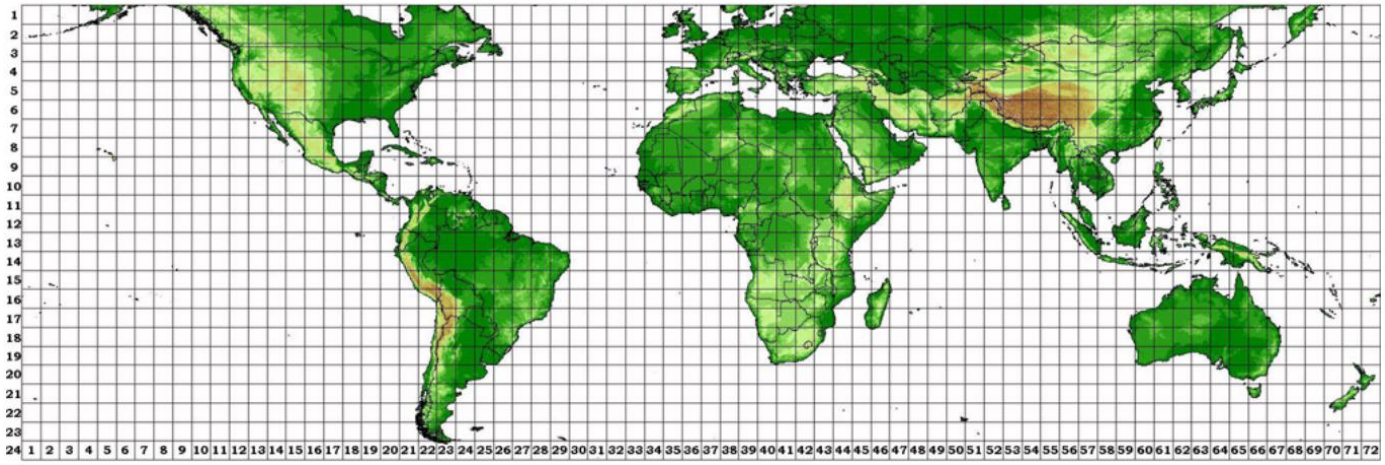

*Figure 2-1 SRTM dataset divided into tiles (http://srtm.csi.cgiar.org).*

## 2.2. Population density

Population density global dataset is provided by Socioeconomic Data and Applications Centre (SEDAC) hosted by CIESIN at Columbia University (Center for International Earth Science Information Network (CIESIN)/Columbia University 2005). Pixel resolution of this dataset is 2.5 arc-minute, which corresponds on approximately to 4.6km. Information about population estimates in years 2010 and 2015 are also available on the website, but for this study a dataset of gridded population in the year 2000 was chosen (see Figure 2-2).

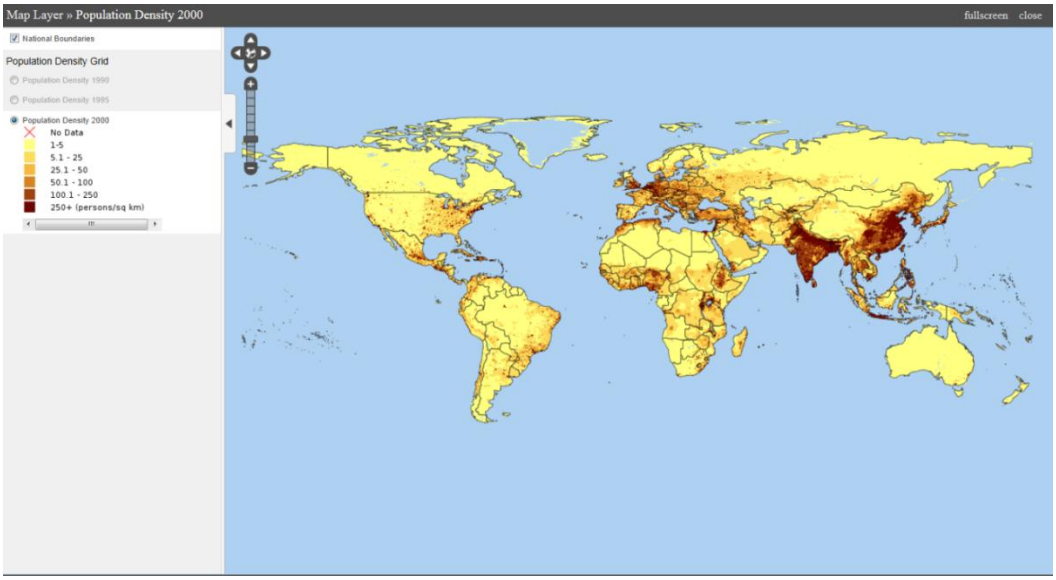


*Figure 2-2 Gridded population density in 2000 (Center for International Earth Science Information Network (CIESIN)/Columbia University 2005)*

## 2.3. Gross domestic product (GDP)

Dataset created by the UNEP (United Nations Environmental Programme) has a grid cell of 30 arc seconds (app. 1km) and it is a compilation of data from various sources (e.g. the World Bank, national GDP data etc.). The unit is estimated value of production per cell in thousands of constant US dollar (from year 2000). Link to the website with the dataset freely available is in Table 2-1.

## 2.4. Geology and soil map

Unfortunately no global geological dataset exists yet in a digital form. Only one portal (www.onegeology.com) offers a global lithological map (1:50 000 000), however no data are available for download. These data would be of very great importance as it could help to estimate the hydraulic conductivity values. The database comprises around 16 000 soil types and is available through server shown in Table 2-1.

## 2.5. Historical tsunami occurrence

Database of historical tsunami events was created by NOAA and includes information about the run-up heights and (see Chapter 3.5) the epicentres of earthquakes causing the tsunami. This data is used as a sort of verification of the estimated vulnerable areas (see Chapter 5).

## 2.6. Meteorological data

A free accessible meteorological data are available through a server listed in Table 2-1, not only precipitation data are available, but also mean, minimal and maximal temperature (not of use in this study). Three main datasets are provided, giving estimates for the future and past conditions, and current (interpolations of measurements in period 1950-2000).

## 2.7. Summary

Table 4-1 gives a list of freely accessible global datasets used in this study. The last two datasets (with *) are likely to be implemented in the future to better estimate the vulnerability on global scale. They weren't implemented in this study due to time limitations.

*Table 2-1 Summary of available data sources, possible implementation in future with **

| Name | Type | Pixel size | Link |
|---|---|---|---|
| SRTM | raster | 90 m | http://www.cgiar-csi.org/data/srtm-90m-digital-elevation-database-v4-1 |
| Population density | raster | ≈ 4.6 km | http://sedac.ciesin.columbia.edu/data/collection/gpw-v3 |
| GDP | raster | ≈ 1 km | http://preview.grid.unep.ch/index.php?preview=data&events=socec&evcat=1&lang=eng |
| Soil map | raster | ≈ 1 km | http://webarchive.iiasa.ac.at/Research/LUC/External-World-soil-database/HTML/ |
| Precipitation | raster | ≈ 1 km | http://www.worldclim.org/current |
| Tsunami occurrence | point shp file | - | http://www.ngdc.noaa.gov/hazard/tsu_db.shtml |
| Bathymetry* | raster | ≈ 1 km | http://www.gebco.net/ |
| Land use* | raster | 300 m | http://due.esrin.esa.int/globcover/ |

# 3. Methodology

## 3.1.General approach

In a study by Sinaga et al. (2011) a case study of GIS mapping of tsunami vulnerability in Bali is carried out. Five variables were used to determine the vulnerability such as the topographic elevation, topographic slope, and topographic relation to tsunami direction, coastal proximity and coastal shape. Different weights are assigned to these variables and a vulnerability index was calculated.

Similar approach is used in this study; however two of those variables are not included in the index calculation. The topographic relation to tsunami is omitted because of a global and general focus of this study and not a regional as in the study by Sinaga et al. (2011). Also the coastal shape is neglected so far because of the global extent and difficulties in its determination for the coasts of the whole world.

## 3.2.Tools

Raster data are processed (resampled, translated into different extensions etc.) through scripts written in Python 2.7 (Appendix 2) and by using the GDAL library (http://www.gdal.org/). GDAL stands for Geospatial Data Abstraction Library and provides tools for manipulation with raster and vector data.

## 3.3. Topographical data

Several studies focused on coastal vulnerability by means of GIS analysis of topographical data used the SRTM; however these studies are on regional scale. (Chandrasekar et al. 2007, McAdoo et al. 2007, Rao et al. 2008) Inaccuracies of the SRTM database might have an effect on a local to regional scale assessment but are suitable for development of a global database with a goal to highlight the most vulnerable areas around the worldwide coasts.

### 3.3.1. Topographical slope

Topographical slope is defined as maximum rate of change in value from a central cell to its neighbours (Cadell 2002). In this study the value is calculated using an utility (gdal_dem) from the GDAL library (http://www.gdal.org/gdaldem.html). It enables to specify the output units (per cent slope or degrees), in this study the slope is expressed in degrees. The GDAL function to calculate the slope uses the Horn's algorithm, which is explained in Figure 3-1.

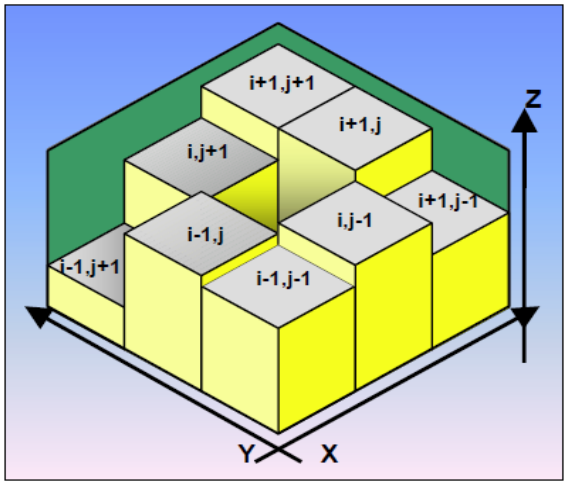


*Figure 3-1 Schematization of the Horn's algorithm, from Cadell (2002)*

The same algorithm is used in the study by Sinaga et al. (2011), where slope for every grid cell is given as:

$$\sqrt{(\delta z/\delta x)^2(\delta z/\delta y)^2} \qquad [3\text{-}1]$$

First term in Equation 3-1 represents angle in east-west direction and the second term angle in north-south direction (Sinaga et al. 2011).

### 3.3.2. Distance to coast

Another important variable for tsunami vulnerability assessment is distance to coast for each pixel of the SRTM dataset. Process of calculating the distance is described in Figure 3-2. Neighbouring tiles have to be also taken into account when calculating a distance to coast for all pixels in a specific SRTM tile. In case the neighbouring tiles are not included in the distance calculation the coastline in adjacent cells might be closer to a pixel form the central cell than the closest coastline of the central cell. This leads to a wrong result (see Figure 3-2b and Figure 3-2c). The script with detailed explanations of the whole distance calculation process is located in a directory specified in Appendix 2.

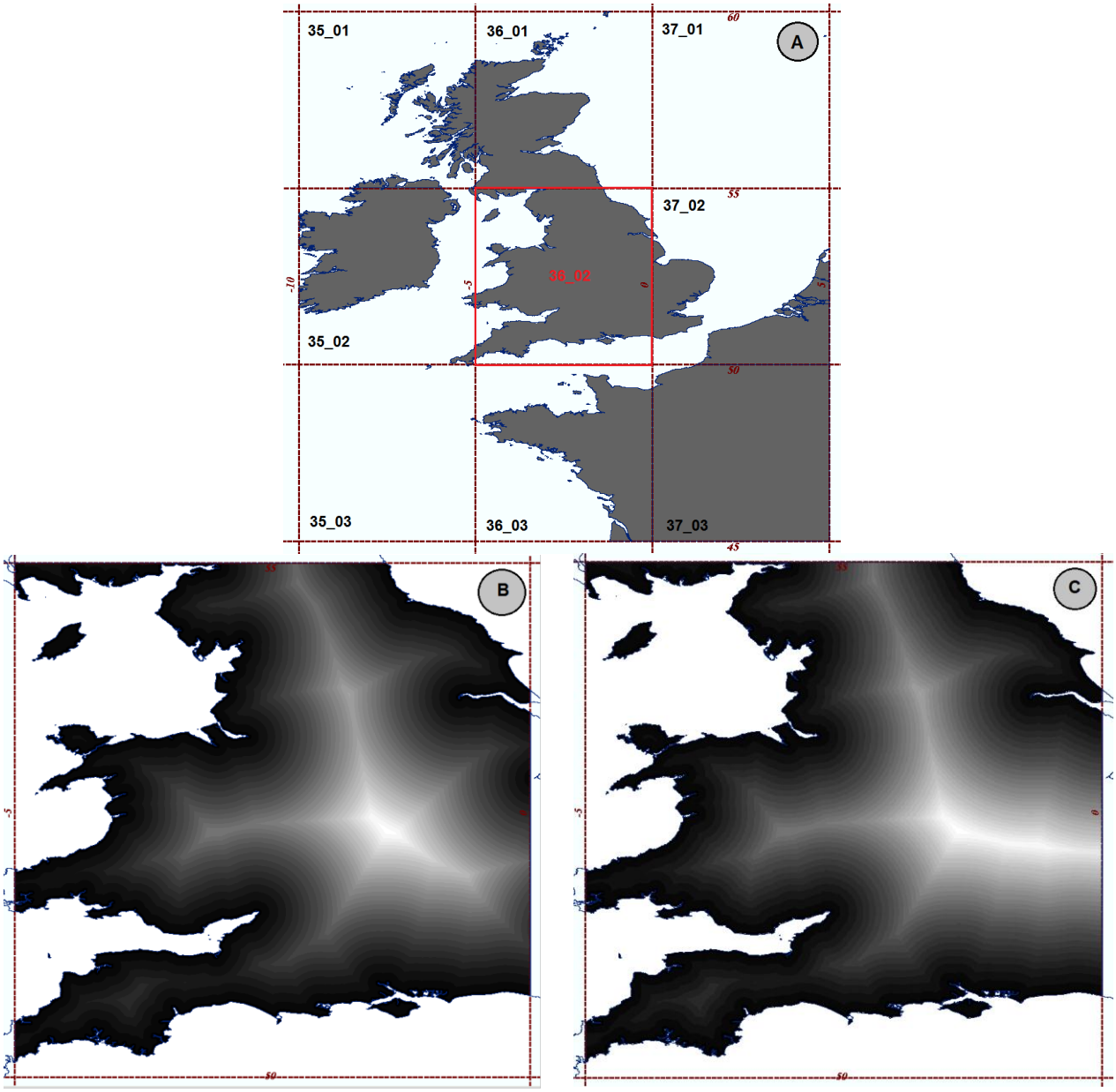


*Figure 3-2 Calculation of distance to coast for the SRTM tile 36_02 (a), the necessity to include neighbouring tiles in the calculation of the distance is clear when comparing the outcome of including the other tiles (b) or not (c).*

## 3.4. Socio-economic data

Apart from topographical data also socio-economic information is valuable to assess the tsunami vulnerability of coastal areas. In this study however, these data can be used for modelling of SWI as parameter values.

### 3.4.1. Population density

Information about population density can lead to estimates of groundwater extraction rates in coastal areas which were highlighted as the most vulnerable zones. As mentioned in Chapter 2.2, population density raster file has a lower resolution than the SRTM. It is also not divided into tiles but gives values for the whole world in only one file. Therefore, cutting and resampling this raster is necessary in order to assign a population density value for each pixel of a SRTM tile. A schematization of this process is shown in Figure 3-3 and a python script used for it is located in a directory specified in Appendix 2. Other necessary data are or can be processed using the same method. No interpolation of values is applied during the resampling process.

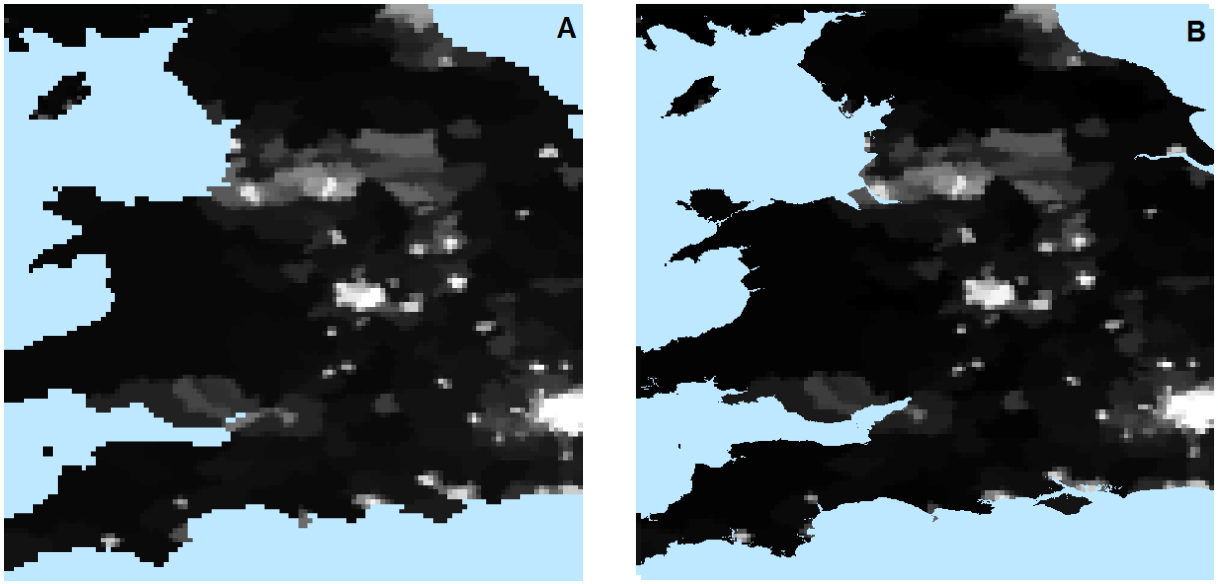


*Figure 3-3 Population density raster cut to extent of the SRTM tile 36_02 (see Figure 3-2), original file (a) and resampled file (b)*

### 3.4.2. Gross Domestic Product

The GDP dataset with a resolution of 1*1km provides global information of income per area ($ per km²). Same procedure as explained in the paragraph 3.4.1 above is applied. Dividing the values of GDP by values of the population density for each pixel (resampled datasets) leads to a GDP value in $ per capita. Having this information, the poorest areas around the world can be selected, with poverty line chosen to be 1$/capita per day.

The poorest places around the world are targeted due to almost no possibilities to find alternative freshwater resources (import from inland, bottled water) after a tsunami event. The procedure of zooming into the most vulnerable areas is described in more detail in paragraph 3.6.2.

## 3.5. Vulnerability index

Several studies dealing with coastal vulnerability to both sea level rise (Diez et al. 2007, Rao et al. 2008) and to natural hazards such as tsunamis Chandrasekar et al. (2007), Szlafsztein et al. (2007) used GIS as an assessment tool.

In the study of (Rao et al. 2008), five physical variables are used to create a “coastal vulnerability index”. These are namely coastal geomorphology, shoreline change, coastal slope, mean spring tide range and significant wave height. However, our study is focused on tsunami vulnerability and therefore the parameters concerning waves and tidal information are not essential and are omitted.

*Table 3-2 Variable values ranges and IDs for the initial vulnerability index*

| ***Initial index*** | **Variable ID values and ranges** | | | | | |
|---|---|---|---|---|---|---|
| **Variable / ID** | **1** | **2** | **3** | **4** | **5** | **15** |
| Topographical elevation (m above sea level) | min - 10 | 10 - 20 | 20 - 30 | 30 - 40 | 40 - 50 | > 50 |
| Topographical slope (°) | 0 - 5 | 5 - 10 | 10 - 15 | 15 - 20 | 20 -25 | > 25 |
| Distance to coast (pixels) | 0 - 10 | 10 - 25 | 25 - 45 | 45 - 80 | 80 - 150 | > 150 |
| Distance to coast (m) | 0 - 900 | 900 - 2250 | 2250 - 4050 | 4050 - 7200 | 7200 - 13 500 | > 13 500 |

*Table 3-1 Final vulnerability indexes calculated as a sum of ID numbers from Table 1.*

| Vulnerability level | Sum of IDs | Vuln. ID |
|---|---|---|
| Very high | 3 - 4 | 1 |
| High | 5 - 7 | 2 |
| Medium | 8 - 10 | 3 |
| Low | 11 - 13 | 4 |
| Very low | 14 - 15 | 5 |
| None | > 15 | 6 |

Another factor which is hard to define on a global scale is coastal geomorphology due to its complexity on a global scale. In this study the vulnerability index is calculated using only three variables, elevation, topographical slope and distance to coast. Ranges are created within values of each variable according to

Table 3-2 and are assigned a value ranging from 1 to 5 (from very high to very low vulnerability) describing the vulnerability of a specific pixel for each variable. When the variable value is out of range (e.g. too far from coast) a value of 15 is assigned. This helps to discard the areas such as moderately elevated plateaus near coasts which might be situated close to the see and have a low topographic slope, but their elevation is higher than potential run-up of a tsunami wave (definition in a paragraph below). These values are then summed for each pixel and a range of values is again implemented, see Table 3-1. By using this procedure, the most vulnerable coastal areas can be highlighted.

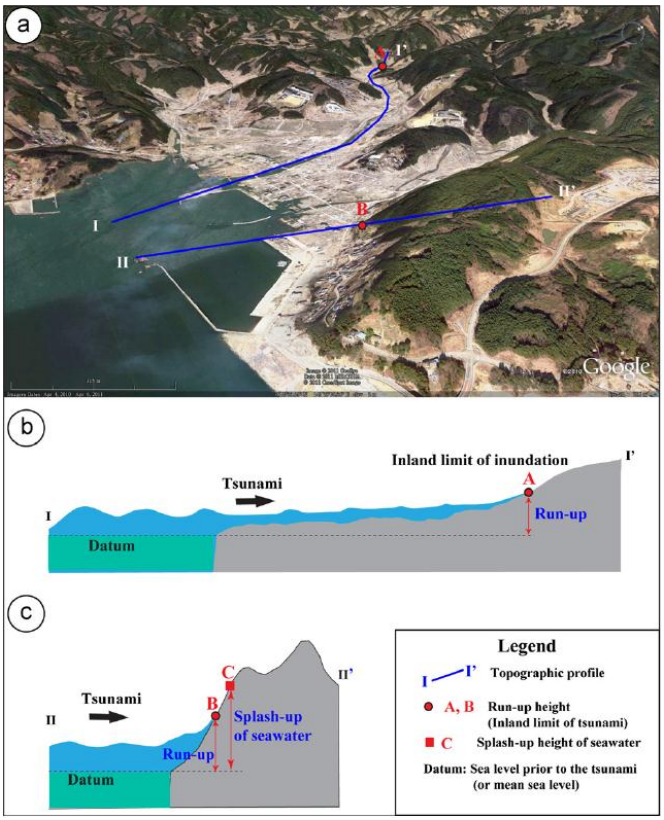


*Figure 3-4 Google Earth image of Minami-sanriku bay area showing two cross-sections (a) and schematization of a run-up in a bay area (b) and on a cliff (c), from Lin et al. (2012)*

Table 3-1 shows only test values to check the functionality of the chosen method. Subsequently ranges of values are varied according to literature and previous studies ((Diez et al. 2007), (Rao et al. 2008), (Sinaga et al. 2011)). Two main designs of the vulnerability index equation are generally applied, sum of weighted variable values ((Rao et al. 2008) and (Sinaga et al. 2011)) or square root of the product of all variable values divided by the count of all variable types (Diez et al. 2007). Rao et al. (2008) suggests that the sum of rank numbers is more responsive to environmental diversity, which is important for our study. Therefore the approach of Rao et al. (2008) is used in this study (sum and multiplication of variables).

To further understand which areas might be more vulnerable to tsunami impacts and how far can tsunami wave reach inland, information from recent tsunami events is useful. Previously mentioned term "run-up" is defined as the inland reach in terms of elevation above sea level (Lin et al. 2012). Figure 3-4 gives an example of run-up and inundation extent of the Minami-sanriku bay area from the study by Lin et al. (2012).

Study of Lin et al. (2012) also suggests that the coastline shape has a large influence on run-up heights and inundation extent and makes a difference between a saw tooth shaped coastline (known as Ria coast) with higher run-up heights and a relatively linear flatter coast with lower run-up heights. Lin et al. (2012) also states that the final run-up height is influenced by bathymetry and amount of co-seismic slip on the source fault, these two parameters are not included in this study.

Other studies (McAdoo et al. (2007), Mori et al. (2011), Shimozono et al. (2012)) focused on measurement and simulation of run-up values and inundation extent for recent tsunami events (Indonesia 2004 and Japan 2011). These studies suggest that the run-up in the flat coastal areas vary between 10 – 15m but can reach more than 30m in the V shaped bays (in the Ria coasts). However these are only approximate values as the run-up heights vary from bay to bay (Shimozono et al.). The study by McAdoo et al. (2007) states that inundation limit on coastal flood plains can reach up to 5km and concludes that tsunami waves rarely transcend areas with slopes greater than 3-4°. Mori et al. (2011) confirms the maximal inundation limit of 5km inland during the tsunami in Japan 2011. This value however depends on the distance from the earthquake epicentre.

Adjusted ranges of variable values according to the information gathered from the studies mentioned above are listed in Table 3-3. Also a new equation (3-2) for the coastal vulnerability index is proposed putting more weight on the topographic elevation is proposed below, as in study of (Sinaga et al. 2011).

*Table 3-3 Ranges of the updated index values and assigned IDs*

| ***Final index*** | **Variable ID values and ranges** | | | | | |
|---|---|---|---|---|---|---|
| **Variable / ID** | **1** | **2** | **3** | **4** | **5** | **30** |
| Topographical elevation (m above sea level) | min - 8 | 8 - 16 | 16 - 24 | 24 - 32 | 32 - 40 | > 40 |
| Topographical slope (°) | 0 - 1 | 1 - 2 | 2 - 3 | 3 - 4 | 4 -5 | > 5 |
| Distance to coast (pixels) | 0 - 7 | 7 - 15 | 15 - 25 | 25 - 40 | 40 - 55 | > 55 |
| Distance to coast (m) | 0 - 540 | 540 - 1350 | 1350 - 2250 | 2250 - 3600 | 3600 - 4950 | > 4950 |

$$vulnerability\ index = 4 * ID_{elev} + ID_{dist} + ID_{slope} \quad [3\text{-}2]$$

By giving more weight to topographic elevation variable in calculation of the updated vulnerability index, range of index values is larger than for the initial index (see Table 3-1). A higher value (30) was assigned to variable values that define areas with no vulnerability at all (see last column in Table 3-3 and last line in Table 3-4). Ranges in Table 3-4 were divided into five equal parts, as in the study of Diez et al. (2007).

*Table 3-4 Vulnerability levels and index values ranges for the updated index*

| Vulnerability level | Sum of IDs | Vuln. ID |
|---|---|---|
| Very high | 6 - 9 | 1 |
| High | 10 - 14 | 2 |
| Medium | 15 - 19 | 3 |
| Low | 20 - 24 | 4 |
| Very low | 25 - 29 | 5 |
| None | > 30 | 6 |

## 3.6. Selection of the most vulnerable areas worldwide

### 3.6.1. Global tsunami hazard

A study by {Finn} assesses a tsunami hazards on a global scale in terms of tsunami event probability and estimates of maximum water level during tsunami inundation (see Figure 3-5). Overlaying Figure 3-5 on top of Figure 2-1 and choosing only areas with estimated water during tsunami inundation level higher than 2m is the first step in narrowing down the most vulnerable areas to tsunamis around the world. This consists in selecting the appropriate tile numbers.

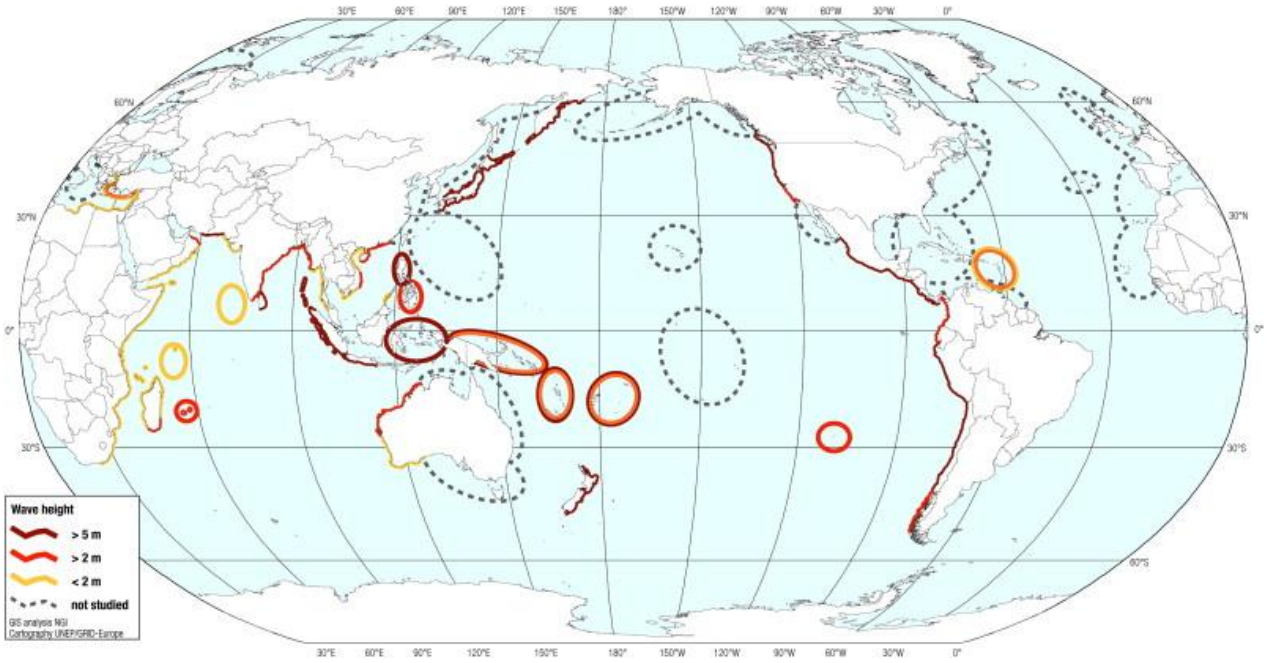


*Figure 3-5 Global tsunami hazard map, with estimates of maximum water level during tsunami inundation* ***{Finn}***

### 3.6.2. Raster masking (overlay)

The procedure described in Paragraph **Error! Reference source not found.**.1 above is a coarse selection of worldwide areas where the risk of tsunamis and potential damage is high, in total 140 tiles were chosen. The next step is to choose the most vulnerable areas in terms of the vulnerability index (see Chapter 3.5) and the poverty rate (see Chapter 3.4). Areas with vulnerability index of 1 (very high vulnerability) and below the poverty line were selected as the most vulnerable overall to tsunami impacts.

A schematization of raster masking is shown in Figure 3-6 and consists in overlaying a number of raster files on top of each other in order to narrow down the areas of interest. The areas in this study are selected according to their vulnerability index value (=1) and GDP (< 1 $/capita per day). By combining these two norms a mask is created (for each tile separately) and is then used to extract parameter value statistics such as soil types, population density and precipitation (see Paragraph 5.2).

Raster masking can be applied to search for different types of areas simply by changing the criteria values or by adding more datasets (increasing the criteria number).

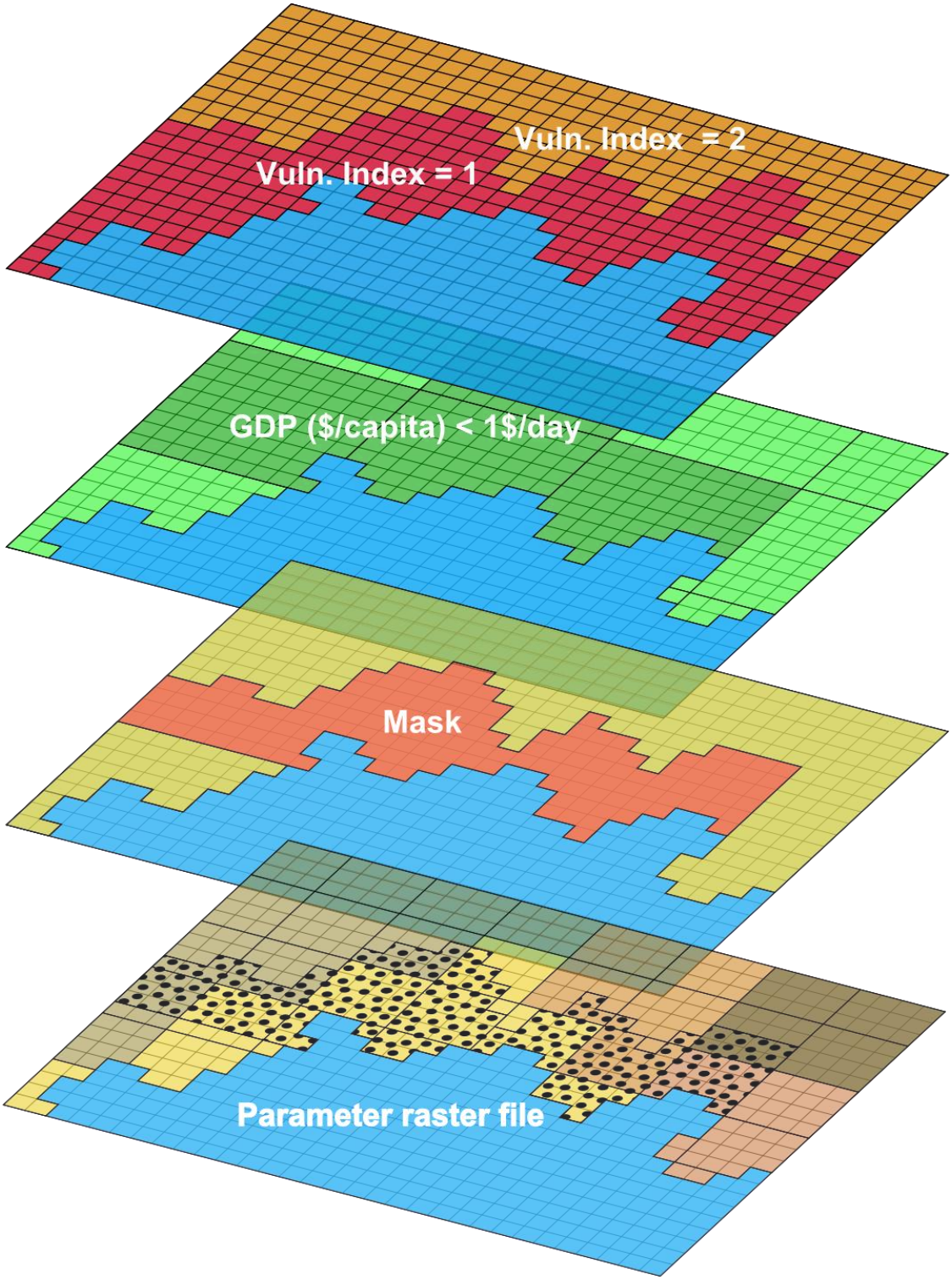


*Figure 3-6 Schematization of raster masking, a method used to select the most vulnerable areas*

## 3.7. Summary

The section above describes the method to assess coastal vulnerability to tsunamis on a global scale. Results for both vulnerability indexes are given in Chapter 5.1 and further improvements of the methodology are suggested in Chapter 7. A schematization of processing the input data step by step until the modeling part is shown in **Error! Reference source not found.**, the green rectangles give names of Python scripts used for a specific process.

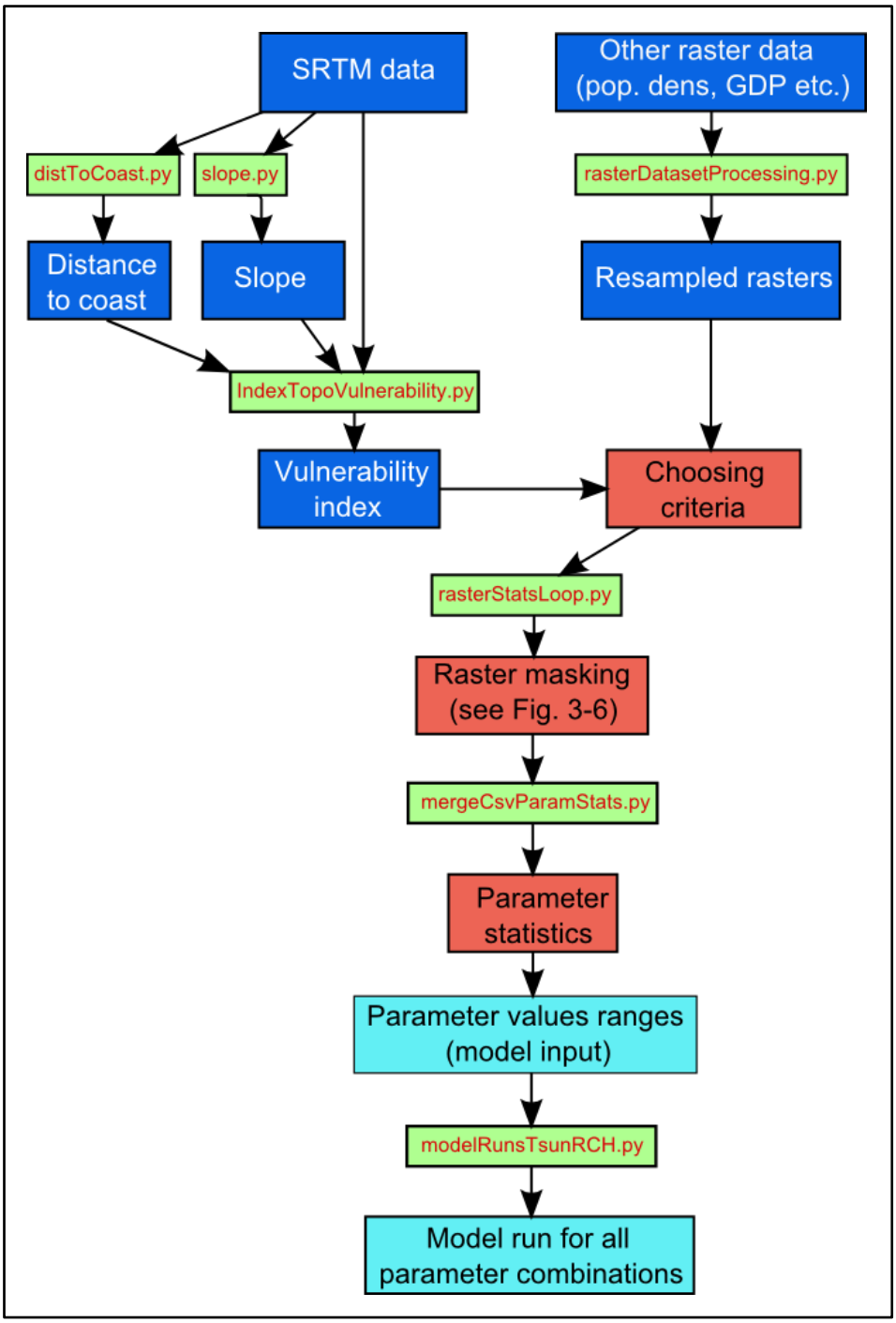


*Figure 3-7 Method schematization, showing step by step the process of finding the most vulnerable areas, extracting parameter (e.g. soil types) statistics and modeling of SWI.*

# 4. Model setup

The chapter below explains the setup of the model starting with a list of input parameter values and followed by a description of the conceptual model and initial conditions.

## 4.1. Input values

Initial model input values are listed in Table 4-1, both constant and variable. The values of water density, molecular diffusivity and longitudinal dispersivity are standard values for density dependent flow modelling. The molecular diffusion (movement of ions) is caused by differences in concentrations and doesn't depend on flow. Including diffusion in the modelling process results in simulating a transition (brackish) zone between the salt and fresh groundwater as diffusion smoothens the concentration gradients. {Oude Essink}

The lower part of Table 4-1 gives a list of variable parameter values. These are based on parameter statistics ranges (recharge, Ksoil, see Figure 5-10), or on estimation (tsunami recharge rate, CHD fresh and K aquifer). Each combination of the variable parameter values represents a different coastal system. A model simulation is performed for all the combinations in order to find the most vulnerable set of parameter values (or coastal system), see paragraph 4.3.

*Table 4-1 Model input parameter values (constant and variable).*

| **Constant parameters** | **Value** |
|---|---|
| Fresh water density (kg/m³) | 1000 |
| Salt water density (kg/m³) | 1025 |
| Molecular diffusivity $D_o$ (m²/s) | 1.00E-08 |
| Longitudinal dispersivity (m) | 1 |
| Soil depth (m) | 1 |
| System length - total (m) | 5 |
| System depth - total (m) | 50 |
| Number of columns | 5002 |
| Number of layers | 53 |
| Soil | 4 |
| Aquifer | 49 |
| Total number of cells | 265106 |
| Number of stress periods | 3 |
| Length of stress period 1 (years) | 200 |
| Length of stress period 2 (hours) | 4 |
| Length of stress period 3 (years) | 75 |

| **Variable parameters** | | | | **Value** |
|---|---|---|---|---|
| | *A* | *B* | *C* | *D* |
| Recharge (fresh) (m/d) | 0.0005 | 0.001 | 0.0025 | 0.005 |
| Tsunami recharge rate (m/d) | 0.5 | 2.0 | 4.0 | - |
| CHD fresh (m) | 0.0 | 5.0 | 15.0 | 30.0 |
| K soil (m/d) | 0.005 | 0.1 | 2.5 | 15 |

| | | | | |
|---|---|---|---|---|
| K aquifer (m/d) | 5.0 | 25.0 | 100.0 | - |

## 4.2. Modeling tools

The computer modeling was carried out using the MODFLOW, MT3D and SEAWAT 4 codes created by the USGS (United States Geological Survey). Scheme of the modeling process is shown in Figure 4-1, with steps done in Python coloured in blue. The parameter combinations and input packages for MODFLOW, MT3D, and SEAWAT are created in Python, specifically the "Flopy" library, which helps to develop Python scripts to run MODFLOW etc. (https://code.google.com/p/flopy/) Python is also used to load in the final head and concentration files and subsequently to create plots and graphs (see Chapter X).

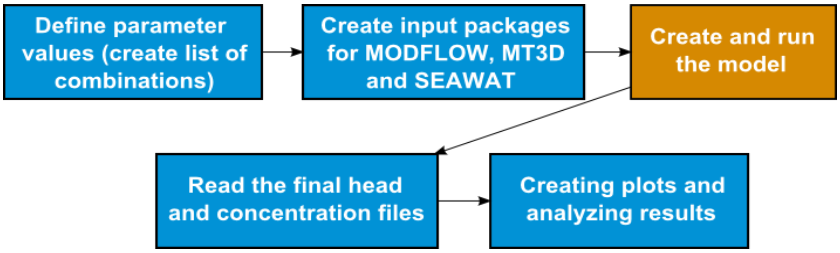


*Figure 4-1 Schematization of the modeling process, steps performed in Python (Flopy library) in blue.*

## 4.3. Conceptual model

Figure 4-2 shows a schematization of the conceptual 2D model, for all three stress periods (from A to C). The first stress period is two hundred years long with a gaol to establish a constant state before the tsunami inundation. During this stress period a constant recharge rate is implemented together with a constant head boundary (CHDfresh in Figure 4-2 to simulate inflow of fresh water into the system. The sea level and inflow of salt water is also simulated as a constant head boundary (CHDsalt). A mixing zone develops with time as an interface between the fresh and salt groundwater. One meter thick layer of soil is situated on top of the aquifer, and has a different hydraulic conductivity value than the aquifer material (see Table 4-1).

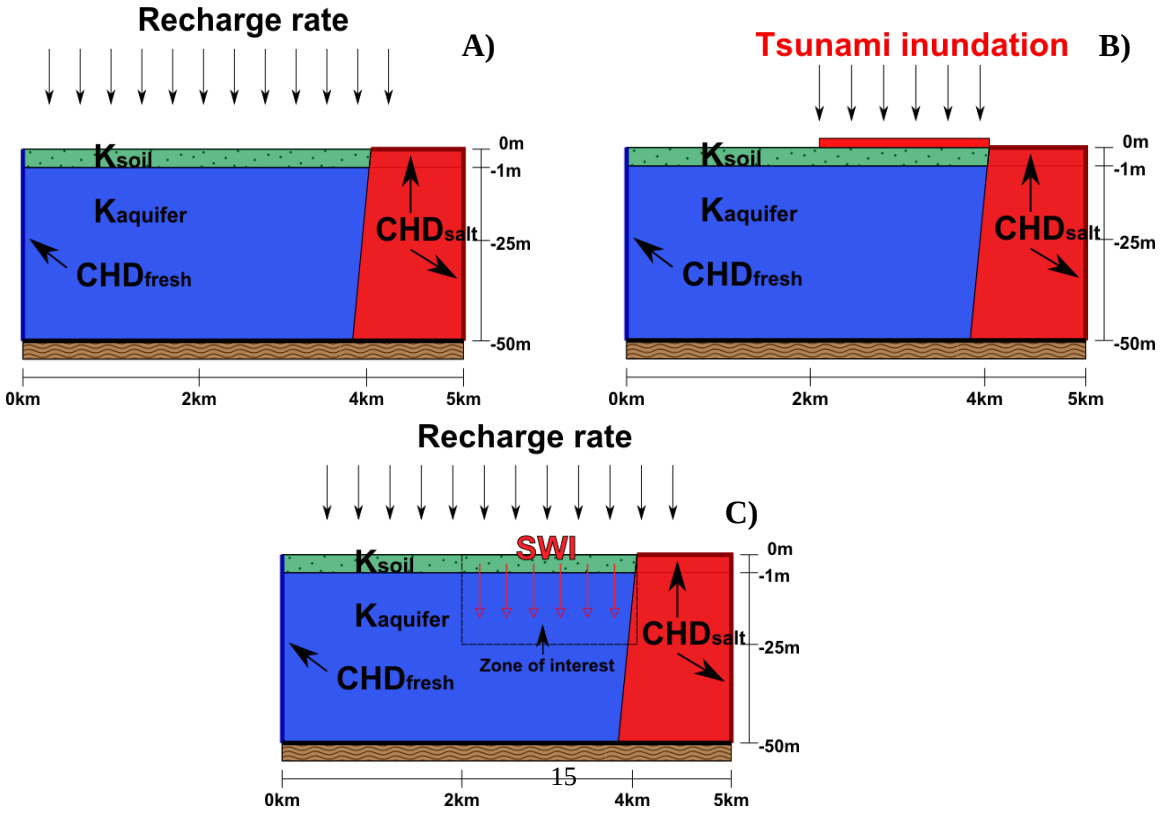




*Figure 4-2 Schematization of the conceptual model for all three stress periods (A to C)*

During the second stress period (see Figure 4-2B) a tsunami inundation lasting four hours is implemented as a recharge of salt water in a limited area, in this case two kilometres inland. The tsunami inundation could be also simulated as a head boundary, which would allow calculating a head for every individual cell depending on distance from coast. In this way, slope effect on the amount of salt water infiltrating the ground could be implemented. Due to time limitations, the easier method (recharge rate) was chosen. Nevertheless, it still provides a good tool to simulate the infiltration of salt water into the ground. It also gives an opportunity to compare the effects of tsunami inundation on different types of coasts (combination of parameter values).

When the tsunami inundation is over, the freshwater recharge rate is set back to the same value as in the first stress period. The last stress period (see Figure 4-2C) lasts 75 years, providing enough time for the infiltrated salt water to get flushed away by the fresh water inflow form the east and by recharge from top. The salt water intrusion (SWI) is observed below the inundated zone (Zone of interest in Figure 4-2C).

Severity of SWI is measured as the amount of time needed for the zone of interest to come back to the same state as before the tsunami (the characteristic time). This is achieved by measuring a number of cells with fresh water concentration (less than 1g of salt per 1l of water) in the zone of interest. When this number exceeds 95%, the state of groundwater is assumed to be as before the tsunami inundation. By comparing the characteristic time of all the simulations a worst case scenarios can be found and linked to their location on a global map.

# 5. Results

This chapter is divided into two sections, the first one describing results of the vulnerability index calculations while the second is focused on results of modeling tsunami induced salt water intrusion modeling. The latter also provides the results of parameter distribution statistics.

## 5.1. Vulnerability index

Results are provided for two areas, namely Spain and Japan, as an example of output from the method described in Chapter 3. The Mediterranean coast of Spain was chosen due to its complex morphology while the coast of Japan (north-western) because of the recent tsunami in 2011 disaster.

### 5.1.1. Spain

Figure 5-1 below shows an example of coastal vulnerability assessment for the coast to south east of Murcia, Spain. Areas in red are the most vulnerable to tsunamis and the light green inland areas have no vulnerability at all. Difference between the extent and size of vulnerable zones suggest different morphology of the coasts, bays with flat plains can be distinguished from cliffs.

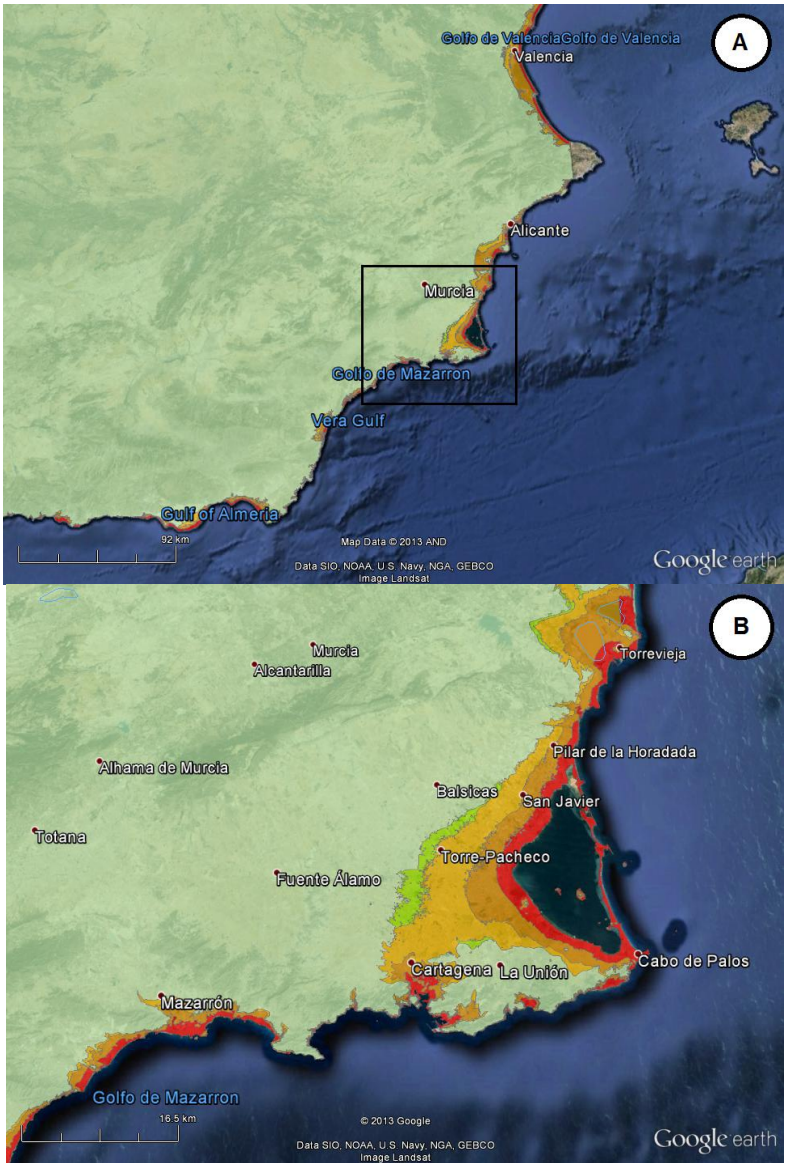


*Figure 5-1 Example of tsunami vulnerability in Spanish Mediterranean coast (a), zoom in nearby Murcia (b), overlay on Google Earth map*

Also in a case of Mallorca difference between cliffs and low laying areas is clear, see Figure 5-2. This figure also shows two measurements of tsunami run-ups; however the scarcity of these measurements of Spanish coast prevents a sort of verification of the highlighted vulnerable zones. Therefore Japan was chosen as another example area for vulnerability assessment and its north-western coast in particular, see Chapter 5.1.2.

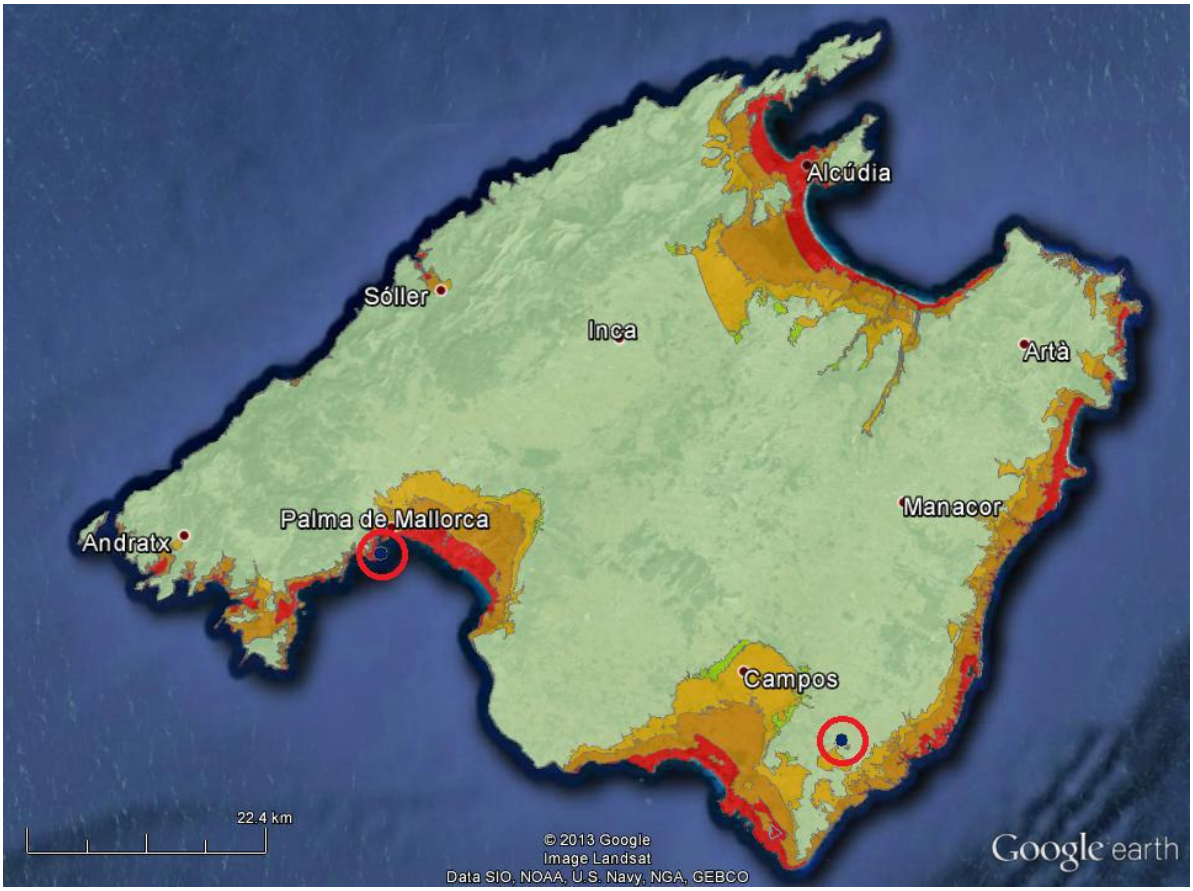


*Figure 5-2 Tsunami vulnerability assessment of Mallorca using the initial index values overlaying the Google Earth map, the points encircled in red represent tsunami run-up measurements from the NOAA database (see Chapter 2.5)*

### 5.1.2. Japan

The western coast of Japan was struck by a devastating tsunami in 2011; mainly affecting the prefectures of Iwate, Miyagi and Fukushima (Mori et al. 2011), see Figure 5-3. Frequent tsunami run-up measurements were gathered after the disaster, e.g. by (Mori et al. 2011) and (Lin et al. 2012), the run-up measurement location and measured values are provided by the NOAA database (see Chapter 2.5).

Two vulnerability indexes are calculated for the same SRTM tile (65_05) covering the coast of the provinces mentioned above, as explained in Chapter 3.5. Vulnerable areas highlighted by the indexes are compared with each other for two types of prevailing coasts, the V-shaped bays (see Figure 5-6Figure 5-7) and flat flood plains (see Figure 5-4Figure 5-5).

Vulnerable areas calculated by both indexes are examined and compared with each other in six areas, see Figure 5-3. Extent of the most vulnerable zones is then compared with the run-up measurements from NOAA database to see if the predicted vulnerable zones match with their location. Two out of the six zones are located in the flood plains (Sendai, Minamisoma), three can be described as V shaped bays (Myiako, Rikuzentakata, Kesennuma) and the last is a river estuary (Kitakami River).

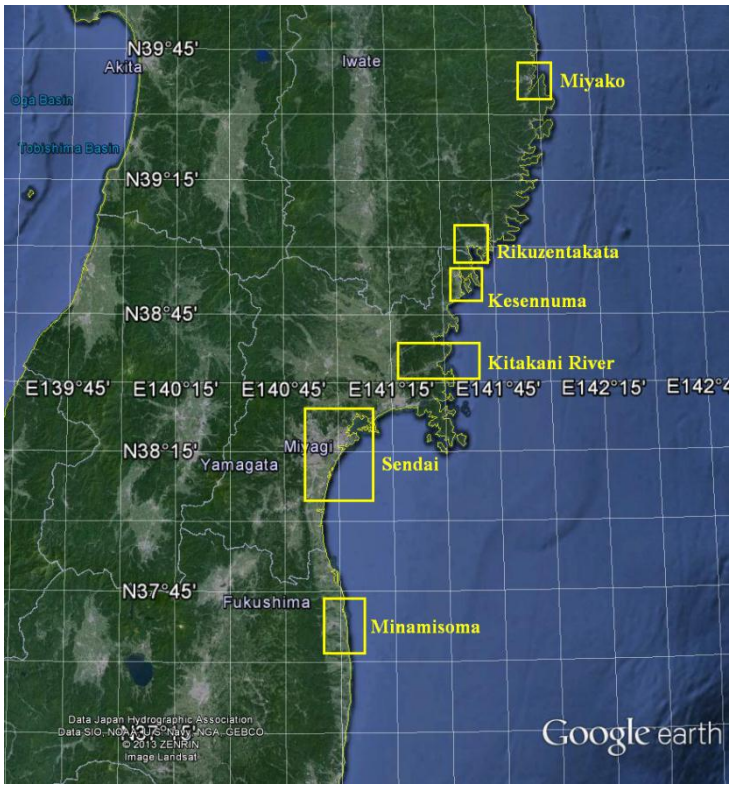


*Figure 5-3 North Western coast of Japan (provinces of Iwate, Miyagi, Fukushima), rectangles represent the areas examined in detail*

Differences in estimation of vulnerable areas between the initial and updated index in a flood plain near Sendai are clear on a first sight. The vulnerable zones estimated by the initial index (see Figure 5-4) stretch far more inland than the zones calculated by the updated index (see Figure 5-5). It is therefore not surprising that the total

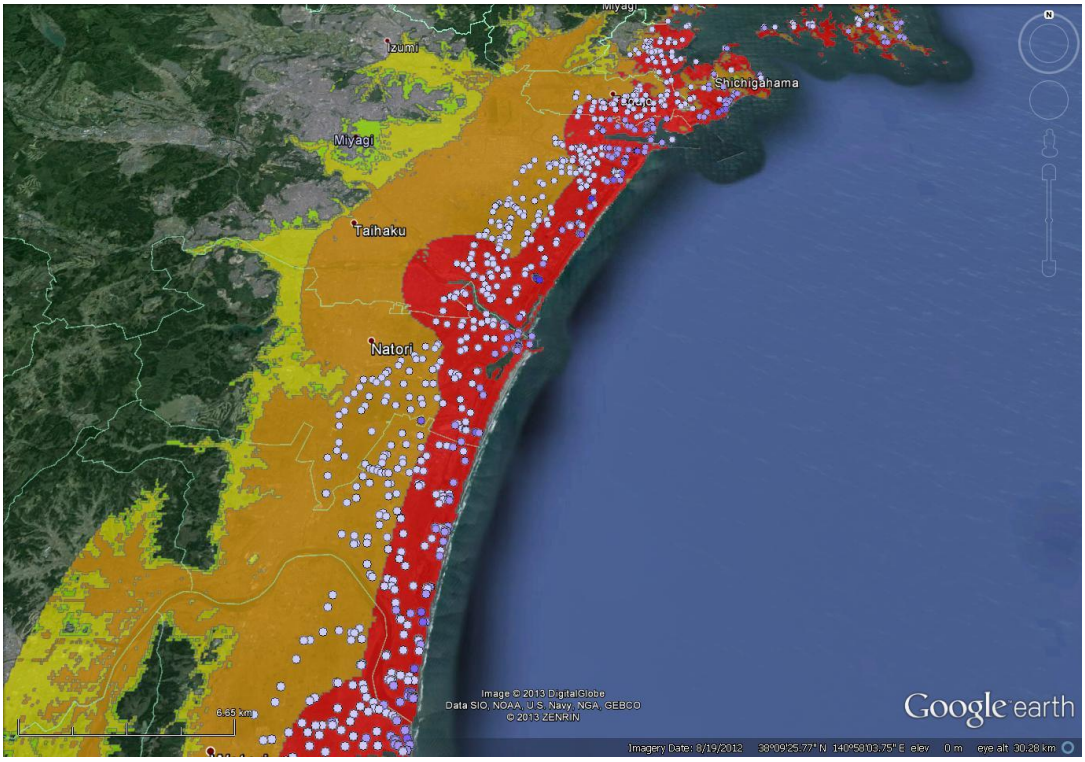


*Figure 5-4 Vulnerable zones near Sendai, initial vulnerability index*

vulnerable area estimated using the initial index covers all the run-up measurements. However, the limit of the estimated vulnerable zones is almost double compared to the distance from coast of the run-up measurements.

The updated vulnerability index provides in general a much better fit to the extent of the run-up measurement locations, see Figure 5-5. Still, two areas seem to either overestimate (1) or underestimate (2) the extent of vulnerable zones.

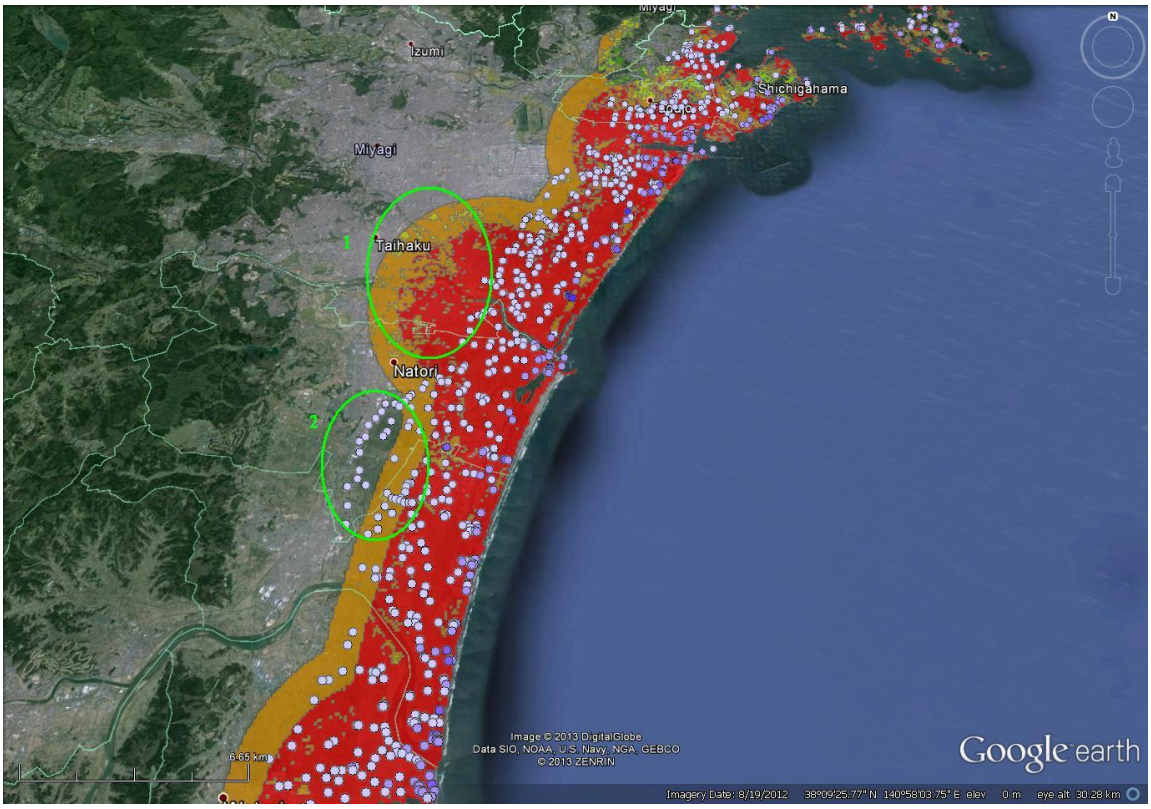


*Figure 5-5 Vulnerable zones near Sendai, initial vulnerability index*

Figure 5-7 and Figure 5-7 show estimated vulnerable zones applying the initial and updated vulnerability index. Same as for the previous case, vulnerable area calculated by the initial index is larger than by the updated index. Nevertheless, the most vulnerable zones stay approximately the same.

Use of the initial index seems to highlight almost the whole shoreline in Figure 5-6, even areas which were not affected by the tsunami (judging from the run-up measurements). On the contrary, vulnerable zones provided by the updated index seem to give quite a good fit with the run-up measurements. Still, some of the areas, especially on the steep slopes where the tsunami splashed up to few tens of meters, seem to be underestimated and are not calculated as vulnerable.

Run-up measurements near the Kitakami River indicate that the tsunami inundation stretched by almost 10km. As the ranges of distance to the coast are limited in the updated index, the vulnerable zones are estimated only in proximity to the shoreline and do not show the more inland areas as vulnerable at all, see Figure 5-8. On the other hand, the estimations given by the initial index cover not only the area with the run-up measurements, but continue farther inland when no inundation occurred, see Figure 5-8.

Figures with the other three cases shown in Figure 5-3 are listed in Appendix 1. They show similar differences and characteristics as described above.

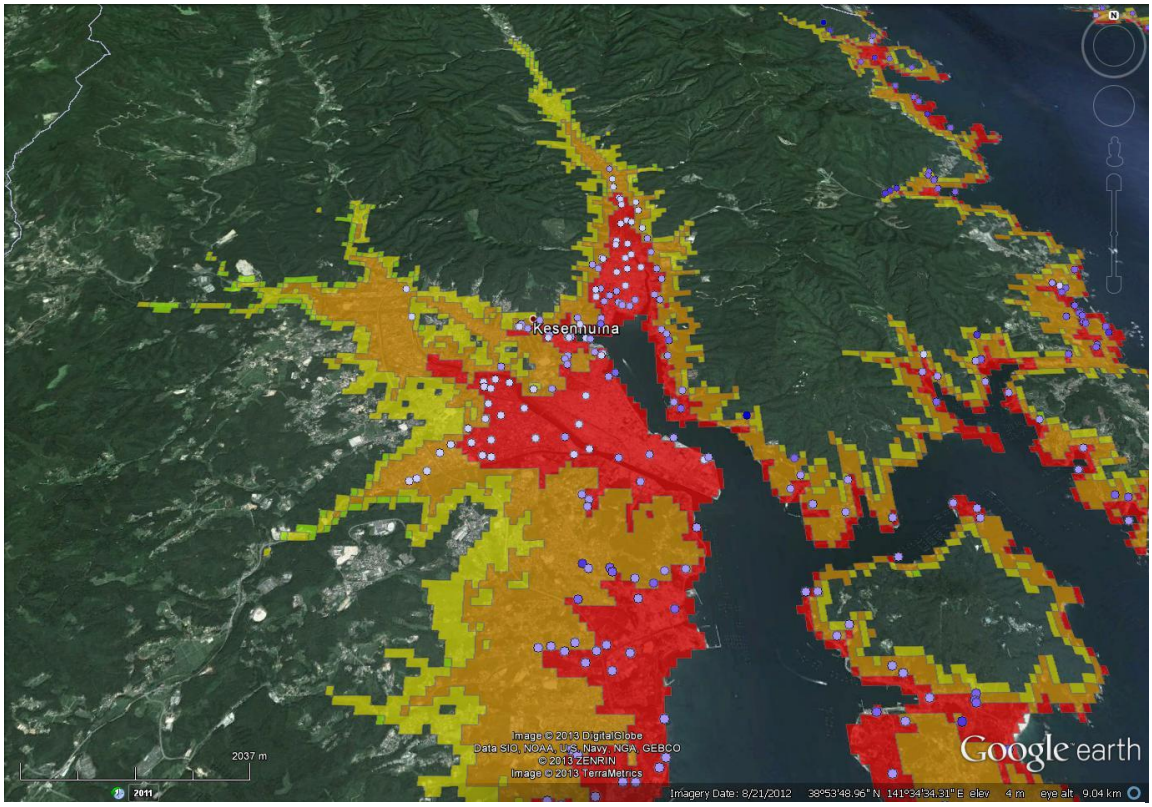


*Figure 5-6 Vulnerable zones near Kesennuma, initial vulnerability index*

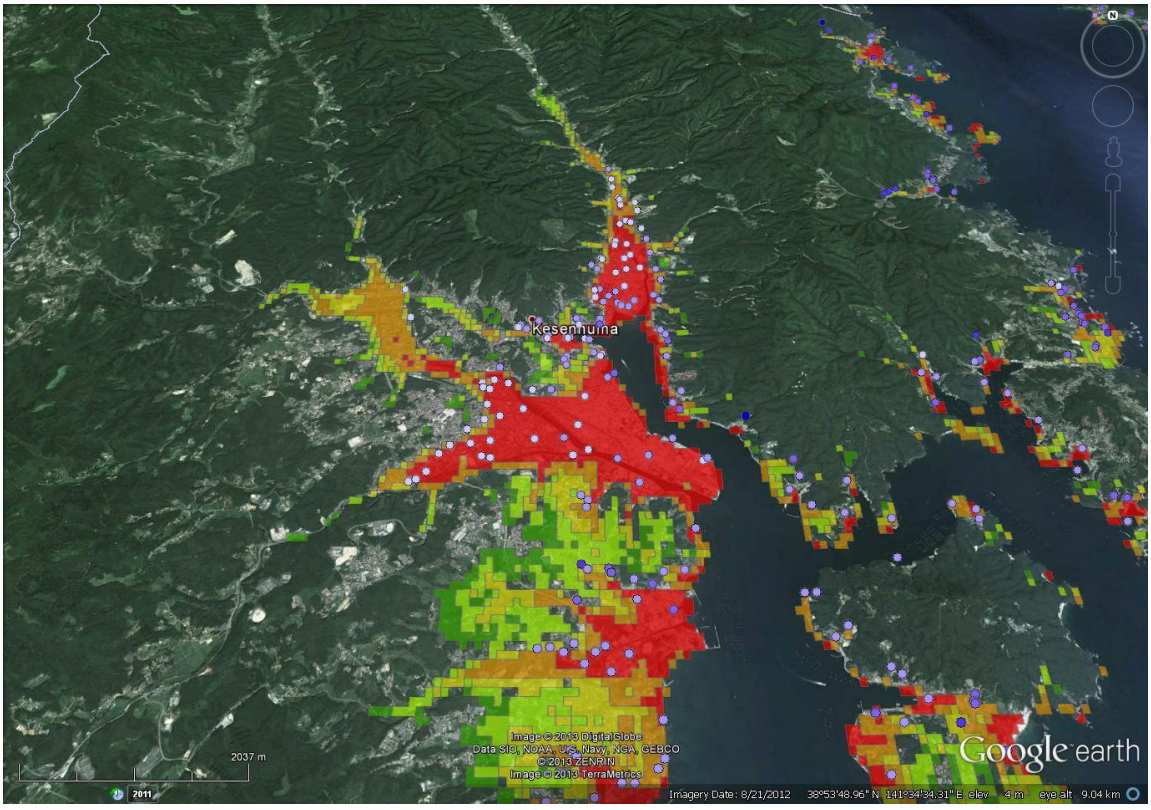


*Figure 5-7 Vulnerable zones near Kesennuma, updated vulnerability index*

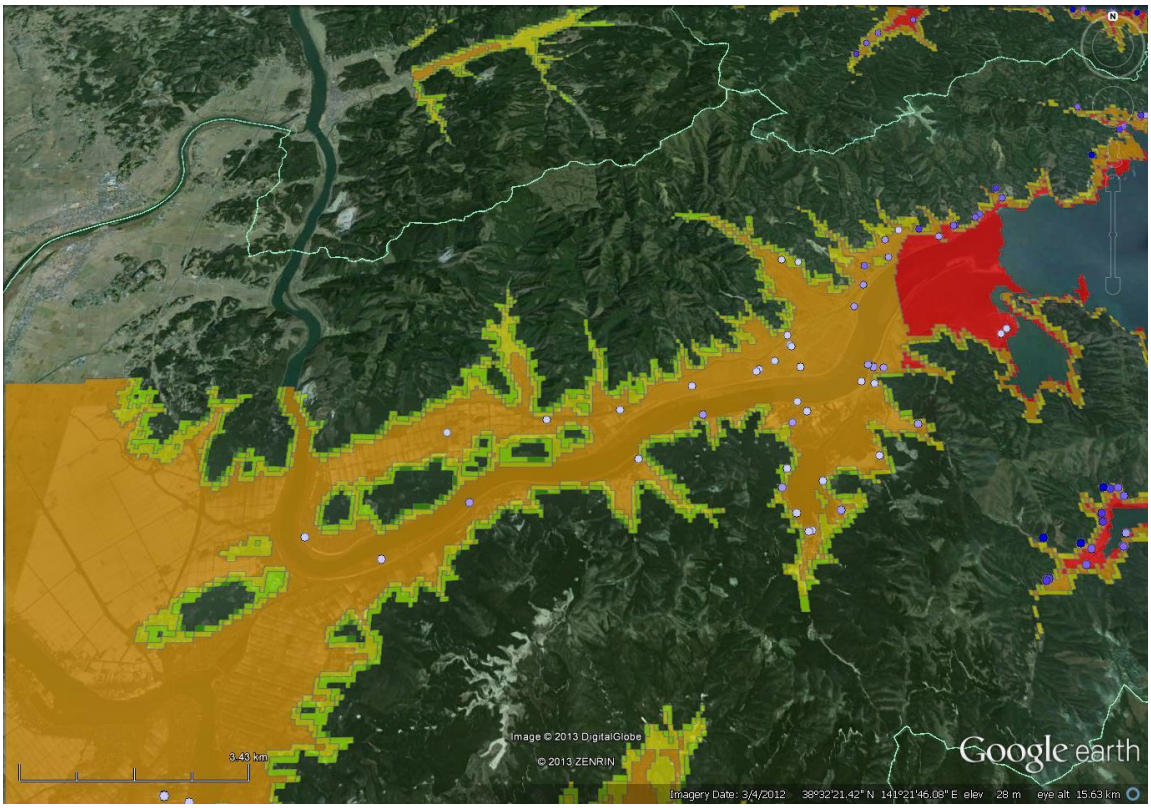


*Figure 5-9 Vulnerable zones near Kitakami River, initial vulnerability index*

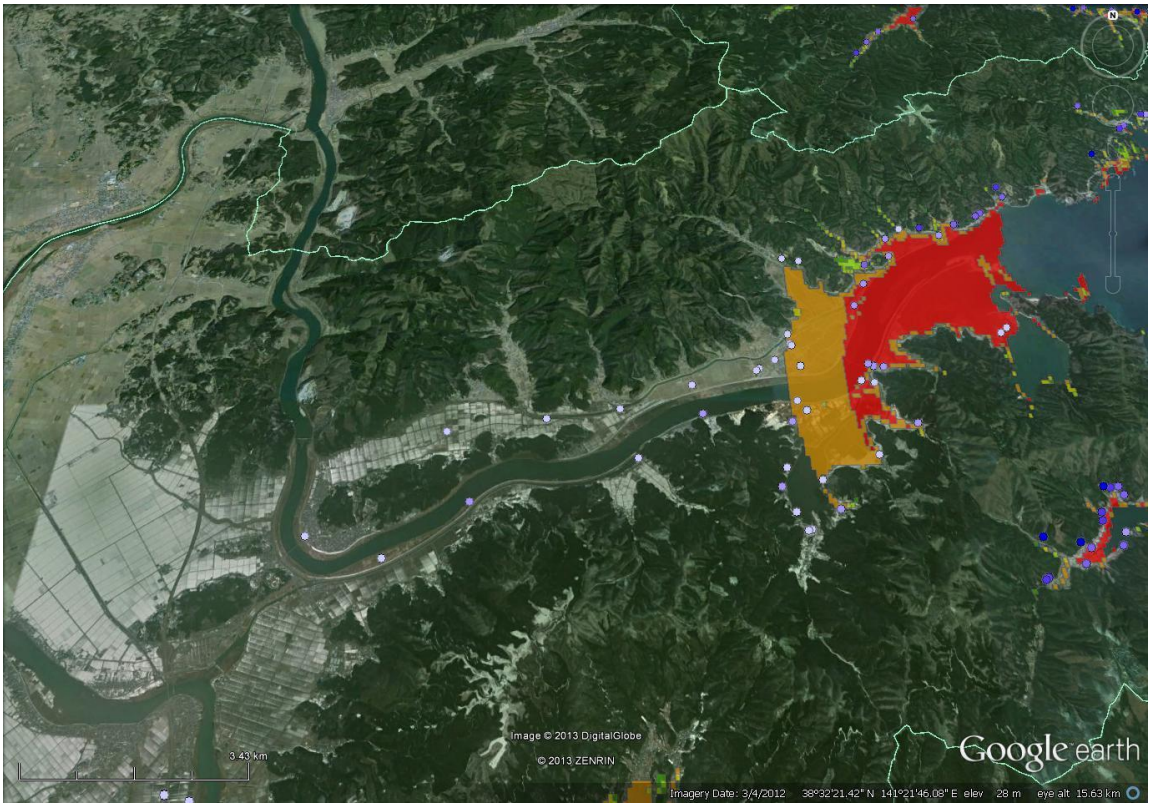


*Figure 5-8 Vulnerable zones near Kitakami River, updated vulnerability index*

## 5.2.Parameter statistics

A link between creating the global vulnerability database and computer modeling of SWI is a distribution of parameter values in the chosen areas (see Chapter 3.6). Histograms of values shown in Figure 5-10 help to determine the variable parameter values given in Table 4-1.

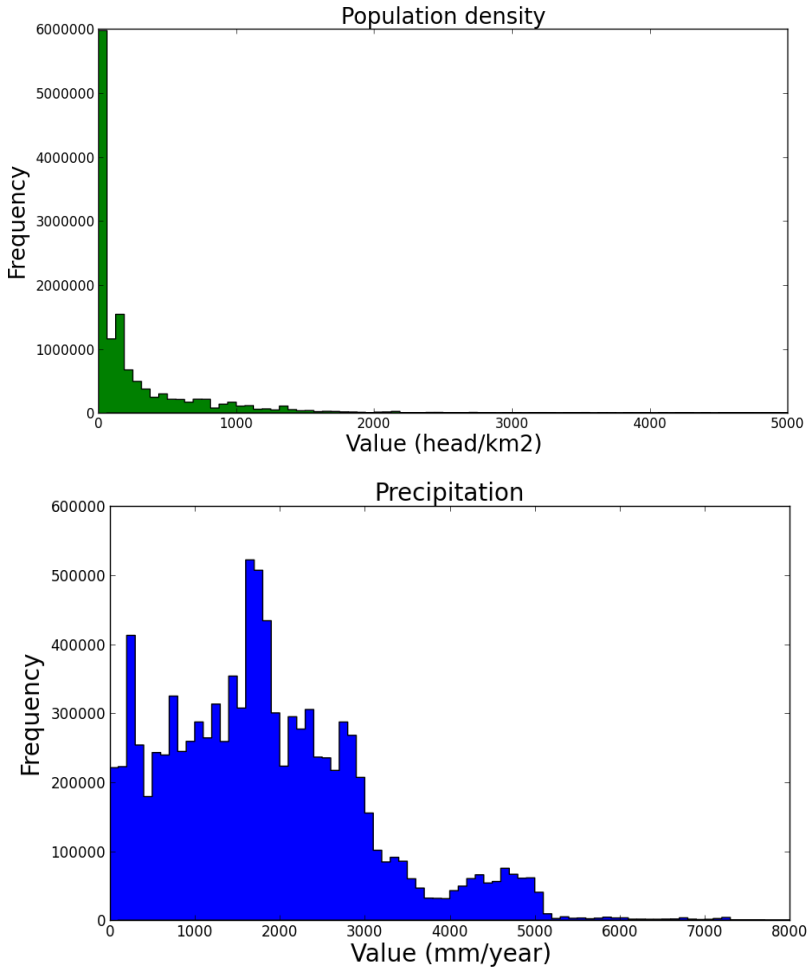


*Figure 5-10 Histogram of parameter values for population density (A), precipitation (B) and soil types (C) for areas selected, see Chapter 3.6*

### 5.3. SWI modeling

# 6. Conclusion and discussion

## 6.1. Conclusions

## 6.2. Discussion

# 7. Recommendations

# 8. References


Cadell, W. (2002). Report on the generation and analysis of DEMs for spatial modelling, March.

Center for International Earth Science Information Network (CIESIN)/Columbia University, a. C. I. d. A. T. C. (2005). "Gridded Population of the World, Version 3 (GPWv3): Population Density Grid.". Retrieved 23/08, 2013, from http://sedac.ciesin.columbia.edu/data/set/gpw-v3-population-density.

Chandrasekar, N., et al. (2007). "Appraisal of tsunami inundation and run-up along the coast of Kanyakumari District, India - GIS analysis." Oceanologia **49**(3): 397-412.

Chidambaram, S., et al. (2010). "Study on the hydrogeochemical characteristics in groundwater, post-and pre-tsunami scenario, from Portnova to Pumpuhar, southeast coast of India." Environmental monitoring and assessment **169**(1-4): 553-568.

Diez, P. G., et al. (2007). "Vulnerability to sea-level rise on the coast of the Buenos Aires Province." Journal of Coastal Research: 119-126.

European Space Agency, E. (2000-2011). "GlobCover project." Retrieved 23/08, 2013, from http://dup.esrin.esa.int/globcover/.

Ferguson, G. and T. Gleeson (2012). "Vulnerability of coastal aquifers to groundwater use and climate change." Nature Climate Change **2**(5): 342-345.

Füssel, H. M. (2007). "Vulnerability: A generally applicable conceptual framework for climate change research." Global Environmental Change **17**(2): 155-167.

G.H.P. Oude Essink and W. v. d. Linden (2005). Impact of the 26-12-04 Tsunami on groundwater systems and groundwater based water supplies, TNO**:** 19.

Hinkel, J. and R. J. Klein (2003). "DINAS-COAST: developing a method and a tool for dynamic and interactive vulnerability assessment." LOICZ Newsletter **27**: 1-4.

Karen G. Villholth and B. Neupane (2011). Tsunamis as Long-Term Hazards to Coastal Groundwater Resources and Associated Water Supplies. Tsunamis - A Growing Disaster. P. M. Mokhtari, InTech.

Lin, A., et al. (2012). "Tsunami run-up associated with co-seismic thrust slip produced by the 2011 M w 9.0 Off Pacific Coast of Tohoku earthquake, Japan." Earth and Planetary Science Letters **337-338**: 121-132.

Løvholt, F., et al. (2012). "Tsunami hazard and exposure on the global scale." Earth-Science Reviews **110**(1-4): 58-73.

McAdoo, B. G., et al. (2007). "Inundation distances and run-up measurements from ASTER, QuickBird and SRTM data, Aceh coast, Indonesia." International Journal of Remote Sensing **28**(13-14): 2961-2975.

Mori, N., et al. (2011). "Survey of 2011 Tohoku earthquake tsunami inundation and run-up." Geophysical Research Letters **38**(null): L00G14.

NASA (2005). "Shuttle Radar Topography Mission, SRTM Mission Statistics." from http://www2.jpl.nasa.gov/srtm/statistics.html.

Rao, K. N., et al. (2008). "Sea-level rise and coastal vulnerability: an assessment of Andhra Pradesh coast, India through remote sensing and GIS." Journal of Coastal Conservation **12**(4): 195-207.

Reuter, H. I., et al. (2007). "An evaluation of void-filling interpolation methods for SRTM data." International Journal of Geographical Information Science **21**(9): 983-1008.

Shimozono, T., et al. (2012). "Propagation and inundation characteristics of the 2011 Tohoku tsunami on the central Sanriku coast." Coastal Engineering Journal **54**(01).

Sinaga, T. P. T., et al. (2011). "GIS mapping of tsunami vulnerability: Case study of the Jembrana regency in Bali, Indonesia." KSCE Journal of Civil Engineering **15**(3): 537-543.

Szlafsztein, C. and H. Sterr (2007). "A GIS-based vulnerability assessment of coastal natural hazards, state of Pará, Brazil." Journal of Coastal Conservation **11**(1): 53-66.

Vafeidis, A. T., et al. (2008). "A new global coastal database for impact and vulnerability analysis to sea-level rise." Journal of Coastal Research: 917-924.

Violette, S., et al. (2009). "Tsunami-induced groundwater salinization in southeastern India." Comptes Rendus Geoscience **341**(4): 339-346.

# 9. Appendix

## 9.1. Estimated vulnerable zones (see Chapter Error! Reference source not found.)

### 9.1.1. Minamisoma

a) Initial index

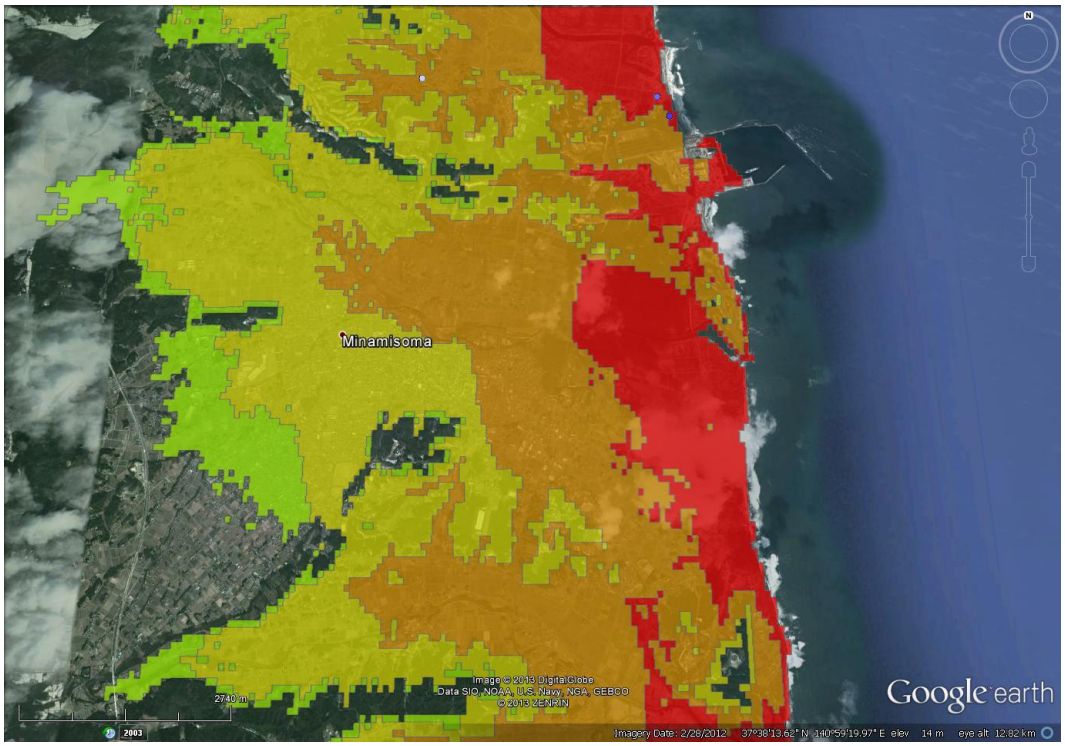


b) Updated index

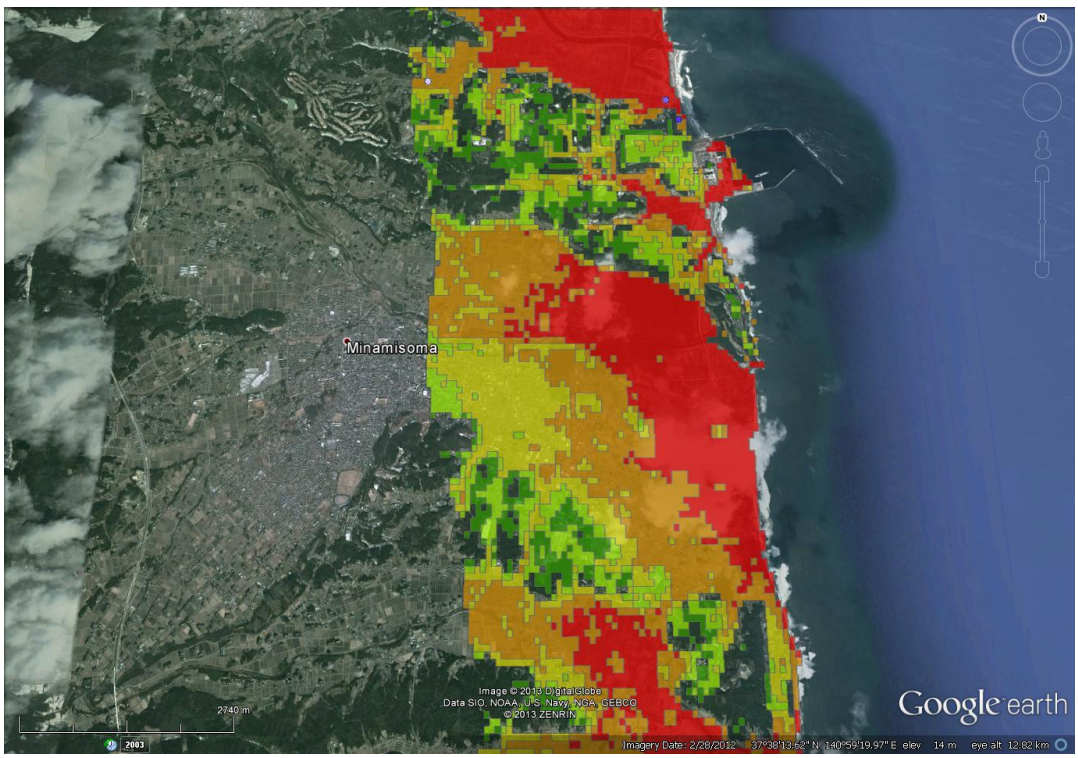

### 9.1.2. Miyako

a) Initial index

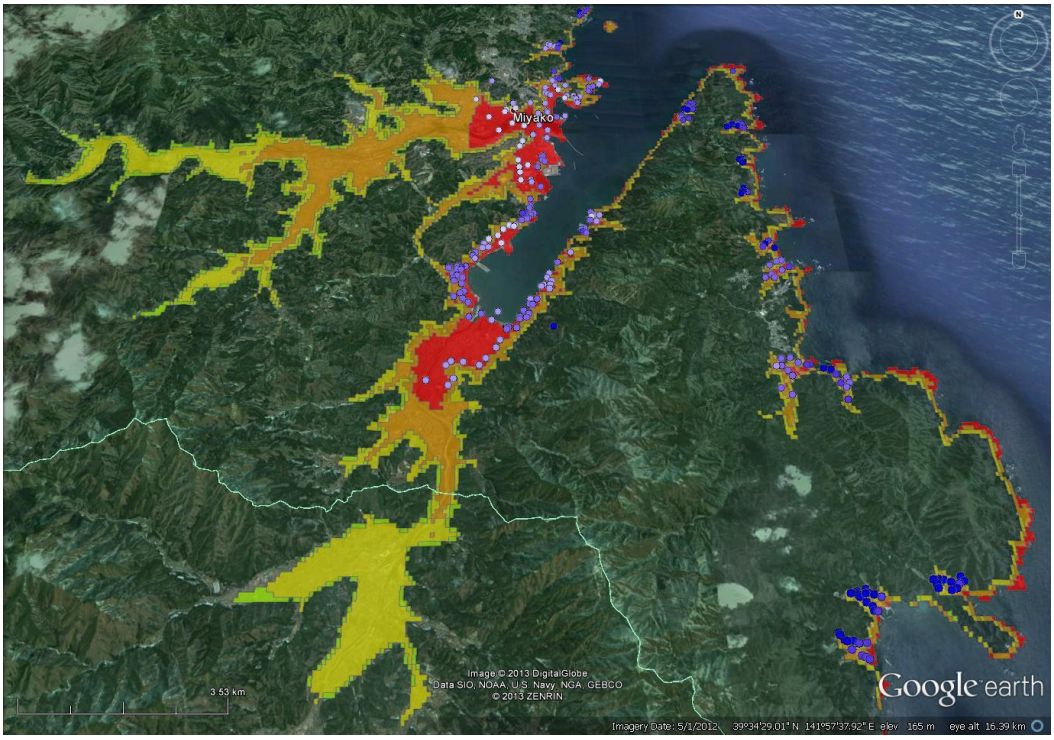


b) Updated index

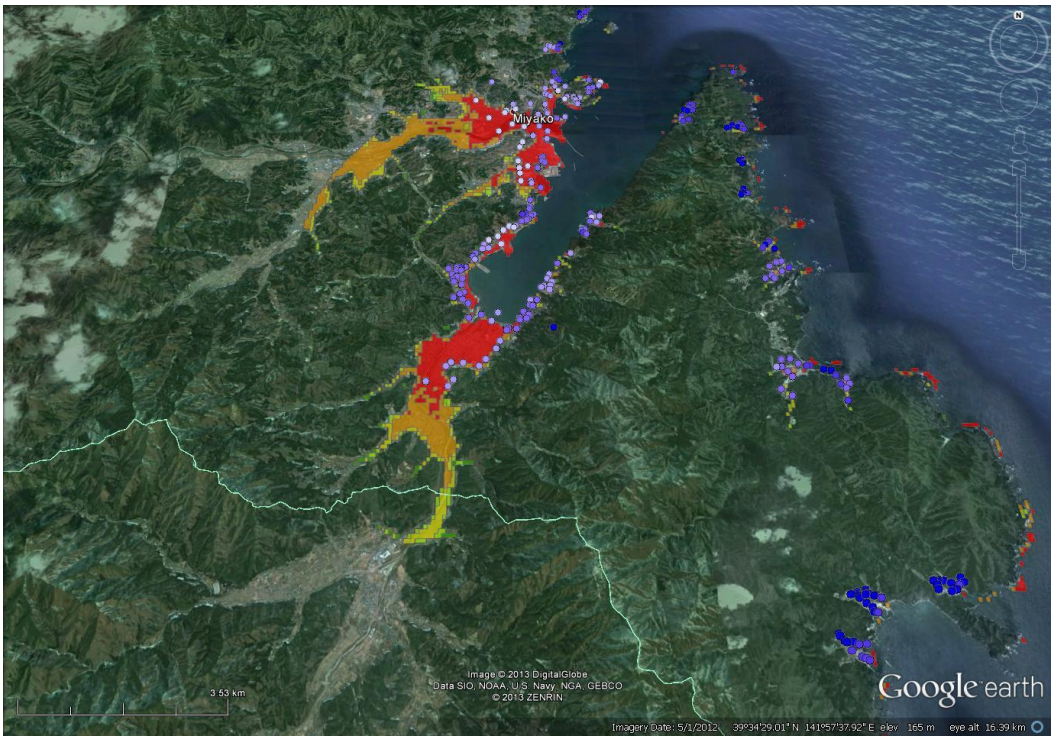

### 7.2.3. Rikuzentakata

a) Initial index

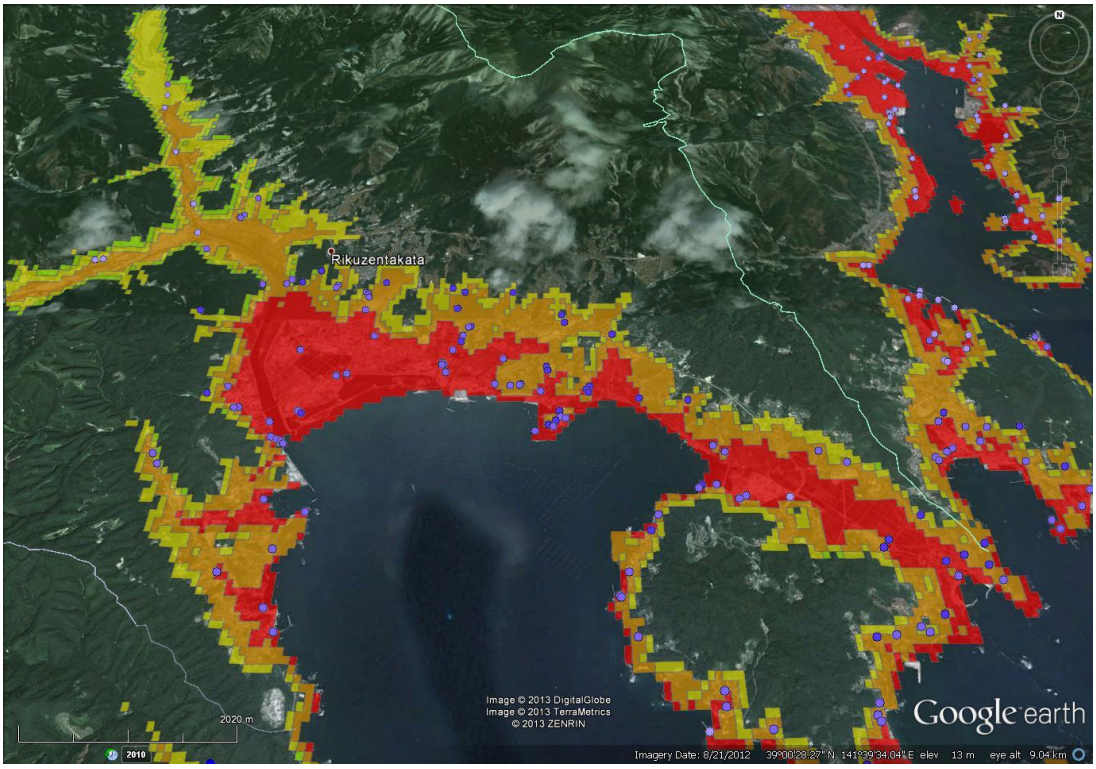


b) Updated index

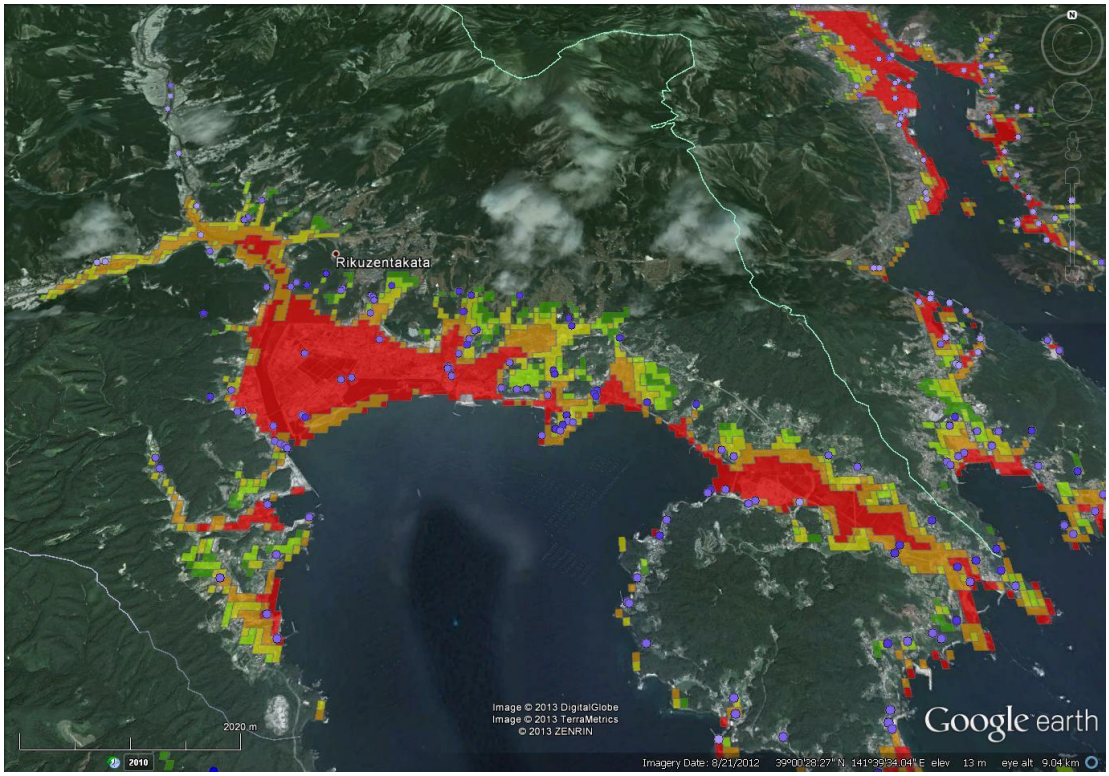

## 9.2. Directory tree

a) Database folder

Main directory (home):

p:\1206381-kvk3-freshwater\communi\studenten\DanielZamrsky\DatabaseData\

Subfolders:

- DistanceToCoast
- Slope
- PopDens
  - Resampled population density raster cut into tiles
- SRTM
  - All SRTM tiles used in the study
- OrigData
  - Original datasets before any manipulation

b) Example, report, scripts

Main directory:

n:\Deltabox\Postbox\Zamrsky, Daniel\tsunamiDtbse\

Subfolders:

- exampleJapan
  - All data for Japan, SRTM, distance to coast, slope, population..
  - Includes calculated index results
  - Not yet all .csv files
- Report
  - Mid-term report
  - Pictures
  - Excel sheet
- Articles
  - All cited articles in this study
- Scripts
  - Python scripts with explanations